



ELSEVIER

Available online at www.sciencedirect.com

SCIENCE @ DIRECT®

International Journal of Thermal Sciences 42 (2003) 141–151

International
Journal of
Thermal
Sciences

www.elsevier.com/locate/ijts

Double diffusive convection in a vertical enclosure inserted with two saturated porous layers confining a fluid layer

R. Bennacer^a, H. Beji^a, A.A. Mohamad^{b,*}

^a *Université de Cergy, Pontoise LEEVAM, Neuville Sur Oise 95031, France*

^b *Department of Mechanical and Manufacturing Engineering, The University of Calgary, Calgary, Alberta, T2N 1N4, Canada*

Received 16 August 2001; accepted 14 March 2002

Abstract

Thermosolutal natural convection in an enclosure filled with fluid and inserted with isotropic or anisotropic porous layers is analyzed numerically. Identical porous layers are attached to the vertical walls, and the walls are held at constant temperatures and concentrations. The horizontal walls of the enclosure are assumed to be adiabatic and impermeable. The aspect ratio of the cavity is equal to two and the saturating fluid is air ($Pr = 0.71$). The analysis is performed for thermal Grashof numbers 10^6 and 10^7 , Schmidt number of 7.1 and for different Darcy number, porous layer thickness and permeability ratio. The results are presented for thermally driven flow, $N = 0$, and for concentration driven flow, $N = 10$. The effect of hydraulic anisotropy on the rate of heat and mass transfer is discussed. It is found that the rate of heat transfer and the rate of mass transfer are weak functions of the Darcy number for high and low permeability regimes. For a certain range of the parameters, the rate of heat transfer decreases when the flow penetrates into the porous layer. Hence, there is an optimum (minimum) value of Nusselt number, which is a function of the anisotropy parameter. Correlation for heat and mass transfer are presented. © 2002 Éditions scientifiques et médicales Elsevier SAS. All rights reserved.

Keywords: Double diffusion; Thermosolutal; Natural convection; Porous media; Multilayer; Anisotropic

1. Introduction

Heat and mass transfer in confined porous media with different configurations have been investigated numerically, theoretically and experimentally due to its importance in many engineering and geophysical applications [1,2]. Natural convection in confined saturated porous media can be classified in two categories: convection in horizontal and vertical enclosures.

The subject of this work is on the heat and mass transfer in a vertical enclosure inserted with isotropic or anisotropic layers of porous matrix saturated with fluid. Buoyancy driven flow by heat and species diffusion is considered. One of the practical motivations of this work arises from the design of building insulation and insulation of heat storage systems. It is common to use layered porous media, with and without an air gap in between the layers, when designing insulators. Moisture or radon migration of other undesirable gas into the insulating layers

is unavoidable under different environmental conditions. Most insulation materials are anisotropic, such as fiberglass, wood etc. Therefore, isotropic modeling of this problem is unrealistic. However, for comparison purposes isotropic media is also considered here. From an engineering point-of-view it is more economical to partially fill the gap of the insulator with porous media. Understanding the process of heat and mass transfer in such systems is important in optimizing the insulator geometry. Another related applications include underground pollution transport and nuclear disposal management, and, heat and mass transfer in human and animals skin. A review of the literature indicated that heat transfer in a vertically layered porous medium was first considered by Poulikakos and Béjan [3]. Their objective was to model inhomogeneity and channeling effects on the heat transfer by considering three layers of porous media with different permeabilities and thermal diffusivities. Lai and Kulacki [4] extended the work of [3] by accounting for layers with different thermal conductivity. The flow within the porous layers was modeled via a Darcy equation in both cases. Hence, the results do not account for the continuity of velocity and shear stress at

* Corresponding author.

E-mail address: amohamad@enme.ucalgary.ca (A.A. Mohamad).

Nomenclature

A	aspect ratio, $= H/L$	X, Z	dimensionless coordinates, $= X^*/H$ and $= Z^*/H$
C	dimensional solute concentration $\text{kg}\cdot\text{m}^{-3}$	<i>Greek symbols</i>	
D	mass diffusivity $\text{m}^2\cdot\text{s}^{-1}$	α	fluid thermal diffusivity $\text{m}^2\cdot\text{s}^{-1}$
Da	Darcy number, $= K_Z/H^2$	β_S	coefficient of volumetric solutal expansion $\text{m}^3\cdot\text{kg}^{-1}$
e	dimensionless gap filled with fluid (without porous material), $= e^*/L$	β_T	coefficient of volumetric thermal expansion K^{-1}
g	gravitational acceleration $\text{m}\cdot\text{s}^{-2}$	ε	porosity
Gr_S	solutal Grashof number, $= g\beta_S\Delta CH^3/\nu^2$	ϕ	dimensionless concentration, $= (C - (C_2 + C_1)/2)/\Delta C$
Gr_T	thermal Grashof number, $= g\beta_T\Delta TH^3/\nu^2$	θ	dimensionless temperature, $= (T - (T_2 + T_1)/2)/\Delta T$
H, L	height and width of the enclosure m	Λ	viscosity ratio, $= \mu_{\text{eff}}/\mu_f$
K	permeability of the porous medium m^{-2}	λ_{eq}	equivalent thermal conductivity $\text{W}\cdot\text{m}^{-1}\cdot\text{K}^{-1}$
K^r	permeability ratio, $= K_X/K_Z$	μ	dynamic viscosity of the fluid $\text{kg}\cdot\text{m}^{-1}\cdot\text{s}^{-1}$
Le	Lewis number, $= \alpha/D$	ν	kinematics viscosity $\text{m}^2\cdot\text{s}^{-1}$
N	buoyancy ratio, $= \beta_S\Delta C/\beta_T\Delta T$	ρ	fluid density $\text{kg}\cdot\text{m}^{-3}$
Nu	average Nusselt number (Eq. (10))	<i>Subscripts</i>	
P	dimensionless pressure	eff	effective
Pr	Prandtl number, $= \nu/\alpha$	f	fluid
Ra^*	Porous thermal Rayleigh number, $= PrGr_T Da$	ref	reference
$\overline{\mathfrak{K}}_{Kr}$	dimensionless tensor of hydraulic anisotropy (Eq. (6))	S	solutal
Sc	effective Schmidt number, $= \nu/D$	T	thermal
Sh	Average Sherwood number (Eq. (10))		
T	dimensional temperature K		
$U(W)$	horizontal (vertical) dimensionless component of velocity, $= U^*H/\nu(W^*H/\nu)$		
\vec{V}	dimensionless velocity vector		

the interface. Other researchers [5–9], investigated natural convection within vertical cavities divided into a fluid layer and a porous layer. Only the heat transfer in homogenous and isotropic porous layer was considered. The main conclusions of the previous studies are that the intensity of the convection is much stronger in the fluid region than in the porous medium region. The degree of fluid penetration into the porous layer increases with increasing permeability and thermal Rayleigh number. It is also found that the rate of heat transfer substantially decreases by attaching a porous layer to the hot or cold wall of the enclosure. The decrease in the rate of heat transfer is very sharp for the porous layer attached to the wall and occupying only 20% of the cavity volume. Further increase in the thickness of the layer does not have a significant influence on the rate of heat transfer. This effect was investigated by Le Breton et al. [10] by attaching a very thin porous layers on the hot and cold walls of an air filled square enclosure. Their results indicated that porous layers having a thickness of the order of the boundary layer thickness are sufficient for the purpose of effective insulation. A similar decrease in mass transfer is noticed by Gobin et al. [11]. They examined the consequence of thermosolutal convection, in aqueous solution, on heat and mass transfer in a confined enclosure partially filled with

an isotropic porous medium. Their results are presented for a buoyancy ratio (solutal to thermal) of 10, aspect ratio of 2, Lewis number of 100 and for Prandtl number of 10. The effect of the porous layer thickness, the Darcy number and the thermal Rayleigh number on the rate of heat and mass transfer was discussed. They found that a relatively thin porous layer has a significant effect on the reduction of heat and mass transfer, as mentioned before. Furthermore, they noticed that the rate of heat transfer decreases as the Darcy number decreases and reaches a minimum value before increasing again. A preliminary explanation of this phenomena was presented in a subsequent publication [12].

The present work analyses the insulating problem and extends the results of [11,12], by considering anisotropic porous layers symmetrically located in an enclosure filled with air. A more extensive explanation of the physics of the minimum in the rate of heat transfer as the porous layer permeability decreases is presented. The effect of attaching porous layers on both vertical walls of an enclosure filled with fluid is discussed on the rate of heat and mass transfer is discussed. A parametric study of the effect of Darcy number, thickness of the porous layers and permeability ratio on the rate of heat and mass transfer is presented.

2. Mathematical formulation

The physical model and coordinate system are shown in Fig. 1. The geometry under consideration is a two-dimensional vertical rectangular enclosure of height H and width L filled with a binary fluid (moist air) and with two identical porous medium layers attached to the walls. The thickness of the fluid layer between the porous layers is denoted by e^* . The vertical walls of the enclosure are subjected to temperature and concentration T_1 and C_1 , at the left wall, and T_2 and C_2 at the right wall. Zero normal temperature and concentration gradients are imposed at the horizontal surfaces. It is assumed that the flow is incompressible, steady and laminar and the binary fluid is Newtonian. The thermophysical properties of the fluid are assumed to be constant, except for the density in the buoyancy term, which depends linearly on both the local temperature and concentration, i.e., the Boussinesq approximation is assumed to be valid,

$$\rho(T, C) = \rho_0[1 - \beta_T(T - T_0) - \beta_S(C - C_0)] \quad (1)$$

where,

$$\beta_T = -\frac{1}{\rho_0} \left[\frac{\partial \rho}{\partial T} \right]_C \quad \text{and} \quad \beta_S = \frac{1}{\rho_0} \left[\frac{\partial \rho}{\partial C} \right]_T$$

Soret and Dufour effects on heat and mass diffusion are neglected. The solid matrix is supposed to be rigid and in local thermal equilibrium with the fluid. The permeability of the porous medium is anisotropic. The principal directions of permeabilities (K_x, K_z) coincide with the horizontal and vertical coordinate axes.

The height of the cavity (H) is taken as a reference length for the spatial coordinates ($X = X^*/H$ and $Z = Z^*/H$), except for the thickness of pure fluid layer which is normalized using the width of the enclosure (L). The reference variables for velocity, pressure, temperature and species concentration are defined as $V_{\text{ref}} = \nu/H$, $P_{\text{ref}} = \rho\nu^2/H^2$, $\Delta T = T_1 - T_2$ and $\Delta C = C_1 - C_2$, respectively.

The Darcy–Brinkman formulation, including the convective inertia term, is adopted in the analysis and we use the one domain approach [13]. The dimensionless macroscopic conservation equations of mass, momentum, energy and species can be written as follow:

$$\vec{\nabla} \cdot \vec{V} = 0 \quad (2)$$

$$\frac{1}{\varepsilon^2} (\vec{V} \cdot \vec{\nabla}) \vec{V} = \Lambda \nabla^2 \vec{V} - \frac{1}{Da} \overline{\overline{\mathfrak{K}}}_{K^r}^{-1} \vec{V} - \vec{\nabla} P + (Gr_T \theta + Gr_S \phi) \vec{k} \quad (3)$$

$$(\vec{V} \cdot \vec{\nabla}) \theta = \frac{1}{Pr} R_\lambda \nabla^2 \theta \quad (4)$$

$$(\vec{V} \cdot \vec{\nabla}) \phi = \frac{1}{Le Pr} \nabla^2 \phi \quad (5)$$

Hydraulic anisotropy of the porous medium is represented by the dimensionless second order tensor:

$$\overline{\overline{\mathfrak{K}}}_{K^r} = \begin{bmatrix} K^r & 0 \\ 0 & 1 \end{bmatrix} \quad (6)$$

where, $K^r = K_x/K_z$.

The dimensionless parameters that characterize the physics of the problem are the aspect ratio of the cavity $A = H/L$, the Prandtl number $Pr = \nu/\alpha$, the Schmidt number $Sc = \nu/D$, the thermal Grashof number $Gr_T = (\beta_T g \Delta T H^3)/\nu^2$ and the solutal Grashof number $Gr_S = N Gr_T = (\beta_S g \Delta C H^3)/\nu^2$. The dimensionless parameters that characterize the flow in porous media are the Darcy number $Da = K_z/H^2$, the ratio of the effective viscosity to the fluid viscosity $\Lambda = \mu_{\text{eff}}/\mu_f$ and the ratio of the fluid thermal conductivity to the porous media effective conductivity ($R_\lambda = \lambda/\lambda_{\text{eff}}$). The porous thermal Rayleigh number is defined as $Ra^* = Gr_T Pr Da$. Hydraulic anisotropy of the porous medium is represented by the dimensionless second order tensor Eq. (6). The analysis is performed for high porosity material and the porosity of the solid matrix appears only in the inertia term. In this case, the inertia term is relatively negligible in porous media. This reason allows us to set the porosity equal to one. We are considering moist air and we set Λ and R_λ to unity, $Pr = 0.71$, $A = 2$ and $Gr_T = 10^6$ and 10^7 .

The boundary conditions for the governing equations are the non-slip condition at the impermeable walls of the enclosure, constant temperature and species concentration at the vertical walls and zero heat and mass fluxes at the horizontal walls of the cavity. Hence,

$$W = U = 0, \quad \theta = 0.5, \quad \phi = 0.5 \quad \text{at } X = 0 \quad (7)$$

$$W = U = 0, \quad \theta = -0.5, \quad \phi = -0.5 \quad \text{at } X = 0.5 \quad (8)$$

$$W = U = 0, \quad \frac{\partial \theta}{\partial Z} = 0, \quad \frac{\partial \phi}{\partial Z} = 0 \quad \text{at } Z = 0 \text{ and } Z = 1 \quad (9)$$

Using the reference diffusive flux $(\lambda_{\text{eff}} \Delta T)/H$ for heat and $(D \Delta C)/H$ for mass, the average rate of heat and mass transfer across the left wall (at $X = 0$) are expressed in dimensionless form by the Nusselt and Sherwood numbers:

$$Nu = \int_0^1 \left(\frac{\partial \theta}{\partial X} \right)_{X=0} dZ \quad (10a)$$

$$Sh = \int_0^1 \left(\frac{\partial \phi}{\partial X} \right)_{X=0} dZ \quad (10b)$$

3. Numerical method

A finite control volume approach is utilized in this work. The set of conservation equations (2)–(5) is integrated over the corresponding control volumes; it leads to a system of algebraic equations. Continuity of the primitive variables and fluxes at the interfaces are insured by a harmonic mean averaging procedure. A classical hybrid scheme is used to approximate the advection–diffusion

terms. SIMPLEC algorithm [14] is utilized for the pressure-velocity coupling in the momentum equation. For high Gr_T , a central difference scheme was also used in approximating advection–diffusion terms. This was done to validate that the present hybrid results are free from numerical diffusion effects. The results were consistent with the prediction of the hybrid scheme.

The resulting algebraic system being solved by the ADI technics. The pressure-velocity interlinking is solved using the SIMPLE algorithm. Numerical experiments were

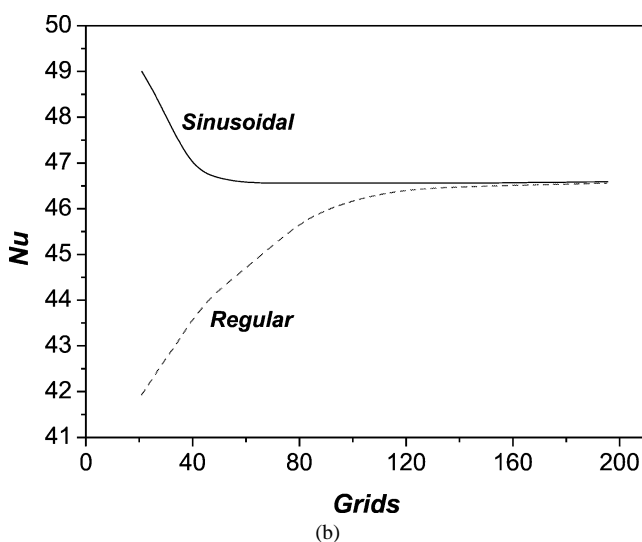
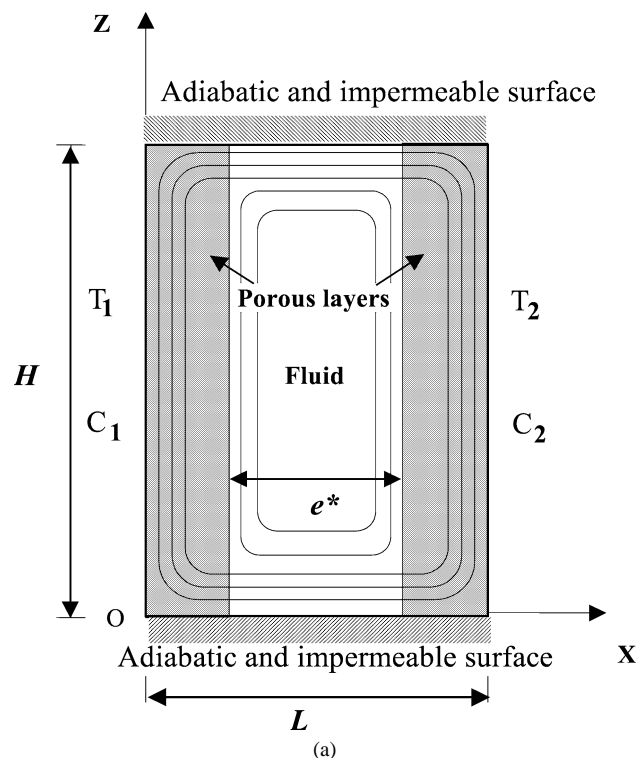


Fig. 1. (a) Schematic diagram of the problem and coordinate system, and (b) the effect of the meshes refinements on Nu ($A = 1$, $Pr = 0.71$, $N = 0$, $Ra^* = 10^4$).

performed to establish that the number and the distribution of the control-volumes are sufficient to resolve the thinnest boundary layer; with more control volumes concentrated near boundaries and at the interfaces (sinusoidal in each layer). In order to ensure that the results are grid size independent, a mesh sensitivity analysis was undertaken and represented on Fig. 1(b). It is found that the irregular grids are necessary. Most calculations presented in this paper were performed using non-uniform 115×145 grids.

The convergence criteria are based on maximum errors in global mass, momentum and energy imbalances. Convergence was insured when the maximum errors become less than 10^{-6} . The code was validated by comparison with the results of Gobin et al. [11] in a composite fluid-porous layer. Details of the numerical validation are reported elsewhere [15].

4. Results and discussions

It is difficult to address the effects of each controlling parameters systematically, when the number of the parameters are quite large. Since, the interest is on the thermal insulation system, the working fluid is air, and hence the Prandtl number is fixed to 0.71. In order to cover all the set of the binary gas and analyze the largest difference in time diffusion, the Schmidt number is fixed to 7.1 in order to get a Lewis number of 10. This Le value allow us to amplify the coupling effect and to cover the order of magnitude of the real Le in binary gases. The results are presented for the cases of the thermal and solutal buoyancy forces aiding each other. The solutal buoyancy force becomes dominant for $N > 1$ and the thermal buoyancy force dominates the flow when $N < 1$. For $N = 0$, the flow is solely driven by the thermal buoyancy force. In the following sections, the numerical results are discussed first considering isotropic layers. The effects of anisotropy on the results are considered in the subsequent section.

4.1. Isotropic layers

Fig. 2 shows the effect of the thickness (isotropic porous layer $K^r = 1$) on the rate of heat (Nu) and mass (Sh) transfers, for a thermally driven flow ($N = 0$) with $Gr_T = 10^7$ and $Da = 10^{-7}$. The figure indicates that the major reduction in the rate of heat and mass transfer takes place when the porous layers occupies about 40% (20% each layer) of the enclosure width ($e = 0.6$). Further increase in the porous layer thickness does not have a significant influence on the transport mechanism. This is true for porous layer thickness equal or greater than the boundary layer thickness [10]. The results are consistent with results of [10,11]. The reason behind the reduction in the rate of heat and mass transfer is that the rate of heat and mass transfer is mainly controlled by the boundary layer thickness. The porous layers add hydraulic resistance to the

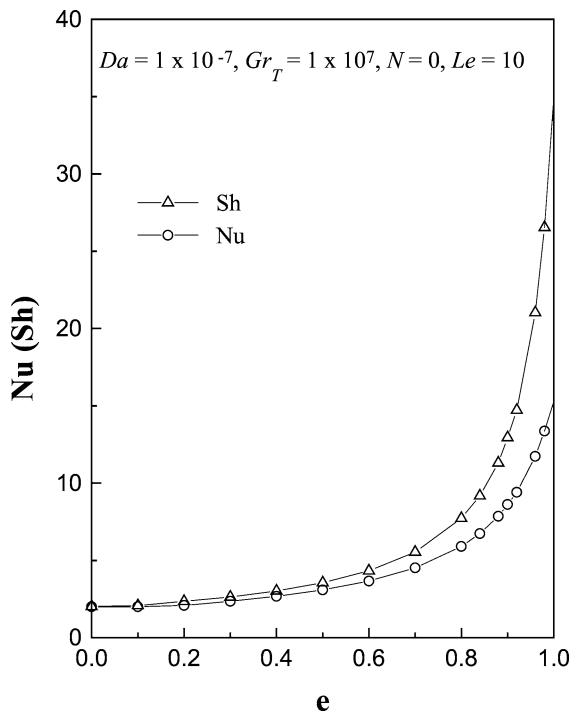


Fig. 2. Nusselt and Sherwood numbers as function of porous layer thickness for thermally driven flow ($N = 0$), $Gr_T = 10^7$, $Da = 10^{-7}$ and $Le = 10$.

boundary layer region. Even though the porous layer may enhance the conduction mechanism, this enhancement does not compensate the reduction in the advection mechanism.

Fig. 3, show streamlines, isotherm and iso-concentration lines for $Gr_T = 10^6$, $N = 10$, $Sc = 7.1$ and $e = 0.8$ and for three regimes of flow in porous layers, i.e., low, intermediate and high permeability regimes. For a low permeability porous layer ($Da = 10^{-7}$), the flow motion is confined to the fluid region and the flow in the porous media is negligible (as seen in Fig. 3(a)). For the same reason the heat and mass transfer in the porous layer are mainly conductive. For intermediate permeability, flow penetration into the porous layers becomes significant (Fig. 3(b)). For high permeability porous layers (Fig. 3(c)) the flow is stronger and is similar to the first case (Fig. 3(a)).

Fig. 4(a), (b) and (c) show velocity, temperature and species concentration profiles at the mid-height of the cavity for $Gr_T = 10^6$, $Sc = 7.1$, $N = 10$ and for different Da numbers, respectively. It is evidence (Fig. 4(a)) that the flow penetration into the porous layer for $Da < 10^{-6}$ is not that significant and the heat and mass transfer in the porous layer are mainly dominated by the conduction mechanism (Fig. 4(b)). Flow penetration increases as Da increases (permeability of the medium increases). It is interesting to note the two peaks in the velocity profiles for $Da = 10^{-5}$, one inside the porous layer and another in the clear fluid region. This can be explained as follows: when the flow penetrates into the porous layer, part of the heat advects vertically and the other part conducts horizontally. The vertical advection mechanism is enhanced

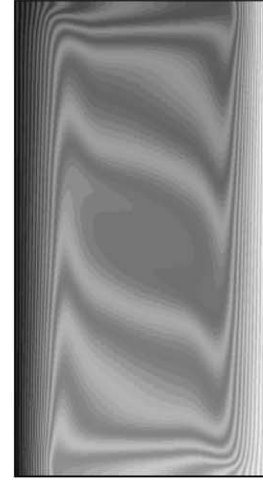
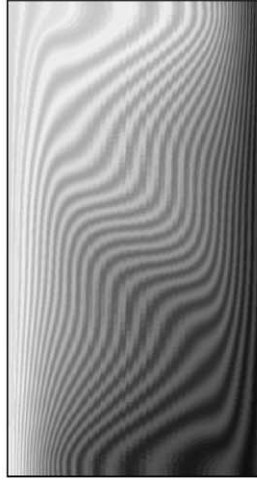
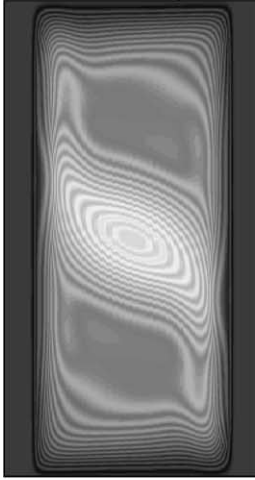
by solutal buoyancy, where the solutal boundary layer is mainly embedded in the porous layer due to the high Schmidt number (Fig. 4(c)). The effect of solutal buoyancy in the fluid region is insignificant as evidence from Fig. 4(c). The species concentration in the clear fluid region is diluted compared with the species concentration in the porous layer region. The horizontally conducted heat warms the clear fluid and induces the buoyancy in the fluid region. Accordingly, the flow in the pure fluid region is mainly thermally driven. As the permeability of the porous layer increases, the heat transfer is predominately by advection and the scale of the horizontally conductive heat decreases. Hence, the peak value in the velocity profile, in the fluid region, starts to diminish as Da increases, i.e., more fluid penetrates into the porous layer.

Temperature profiles at the mid-height of the cavity are shown in Fig. 4(b). For low Da ($Da < 10^{-6}$), the heat transfer in the porous layer is mainly conductive and the temperature profile is linear. As the permeability increases, the flow penetrates into the porous layer, the slope of the temperature profile decreases and consequently the rate of heat transfer decreases (Fig. 5). This is evidence in Fig. 4(b) by comparing slope of the temperature profiles for $Da = 10^{-6}$ and $Da = 5 \times 10^{-5}$. As mentioned before, the decrease in the rate of heat transfer by increasing the permeability of the porous layers is due to the decrease in the rate of horizontal conductive heat transfer, which reduces the intensity of the flow (buoyancy) in the pure fluid region. Hence, an increase in the advection mechanism in the porous layer (enhanced by solutal effect) does not compensate the decrease in the rate of the heat transfer in the pure fluid region. Therefore, the total rate of heat transfer decreases.

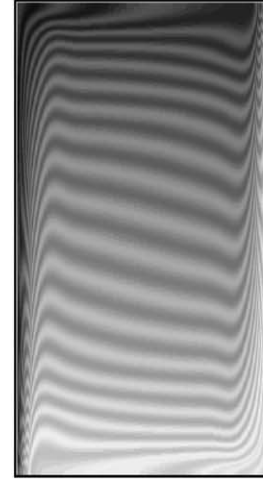
From the above it becomes clear that the minimum rate of heat transfer should also be a function of the porous layer thickness (this issue will be discussed later, Fig. 6(a)). Further increases in the permeability, enhances the advection in the porous layer and results in increases of the rate of heat transfer—notice the increase in the temperature profile slope for $Da > 10^{-4}$. This case corresponds to one main circulation in the entire enclosure as shown in Fig. 3(c). Fig. 4(c), shows concentration profiles for different Da . The solutal boundary layer is thinner than the thermal boundary layer because the Schmidt number is set to be higher than the Prandtl number ($Le = Sc/Pr > 1$). It should be mentioned that the ratio of the thermal to solutal boundary layers is proportional to Le [16]. No inversion in the slope of species concentration is evidence in Fig. 4(c). Sh monotonically increases as Da increases for the intermediate permeability values, see Fig. 5.

The effects of the porous layer thickness on the rate of heat and mass transfer are illustrated in Fig. 6(a) and (b), respectively. For a high permeability porous layer ($Da > 10^{-3}$), the existence of the porous layers do not influence the rate of heat and mass transfer significantly, especially the rate of mass transfer. For $Da < 10^{-3}$ the rate of heat

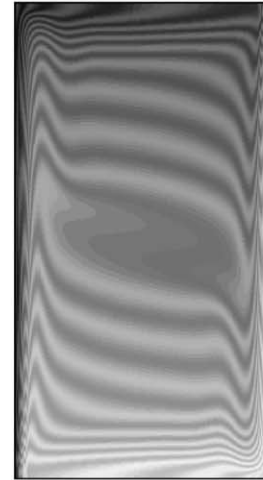
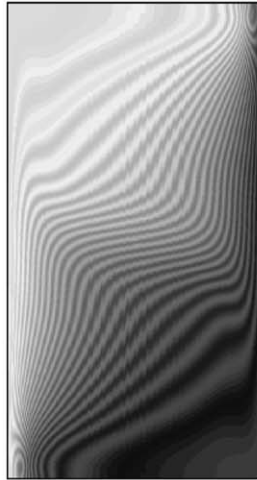
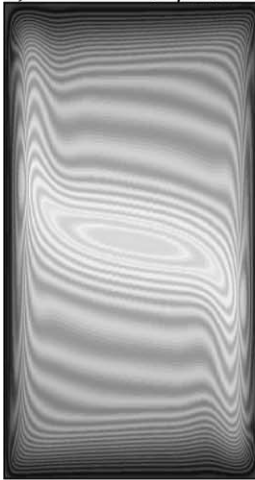
a) $Da=10^{-7}$, $\psi_{\max}=7.90$



b) $Da = 10^{-4}$, $\psi_{\max}=6.19$



c) $Da=10^{-2}$, $\psi_{\max}=12.17$



Streamlines

Isotherms

Isoconcentration lines

Fig. 3. Streamlines, Isotherms and Isoconcentration for $Gr_T = 10^6$, $N = 10$, $Le = 10$, $e = 0.8$ and for (a) $Da = 10^{-7}$, (b) $Da = 10^{-4}$, and (c) $Da = 10^{-2}$.

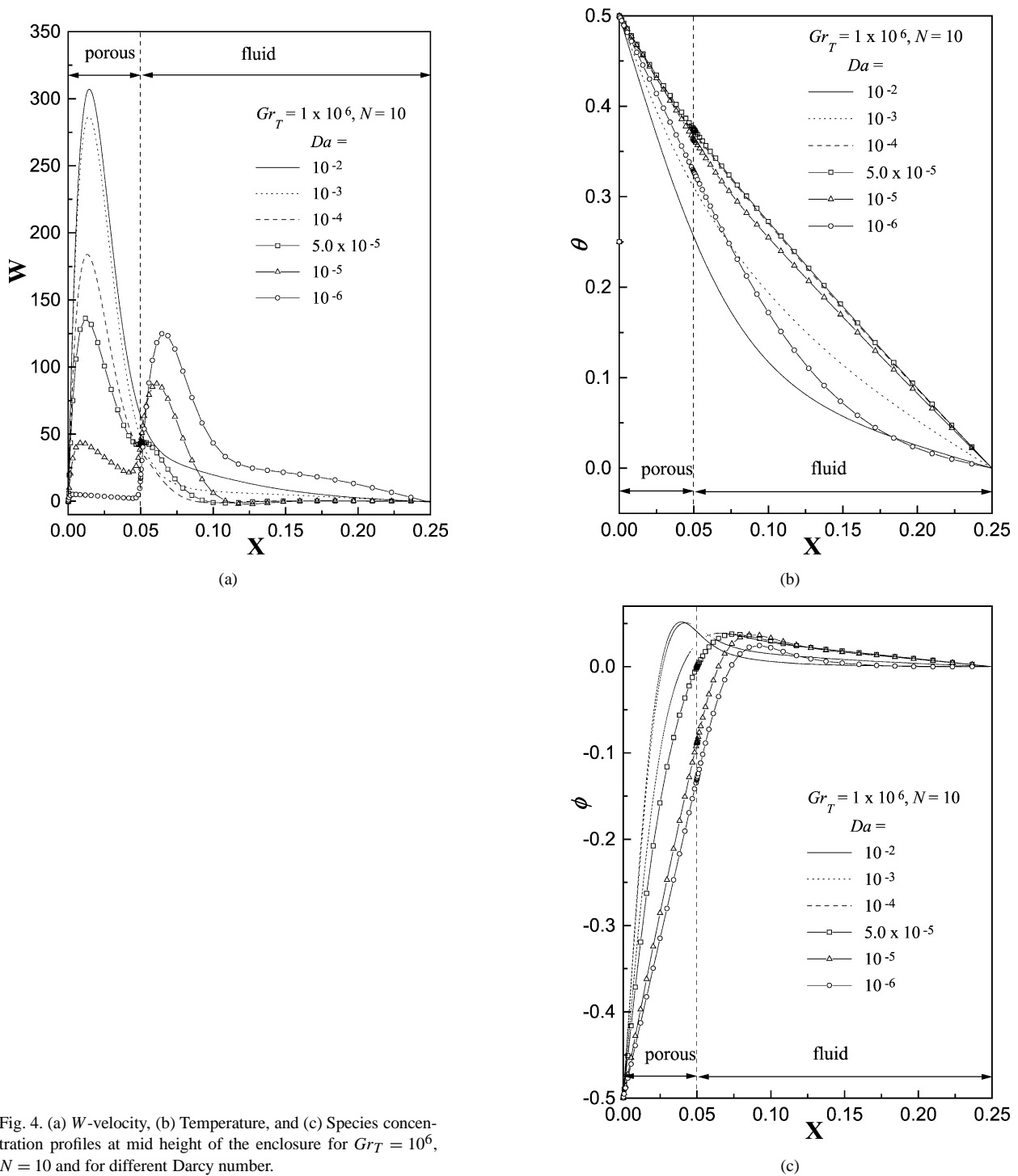


Fig. 4. (a) W -velocity, (b) Temperature, and (c) Species concentration profiles at mid height of the enclosure for $Gr_T = 10^6$, $N = 10$ and for different Darcy number.

and mass transfer decreases by increasing the porous layer thickness. The rates of heat and mass transfer decrease significantly for porous layer thickness from 0 to 0.2 (e from 1 to 0.8). Further increases in the porous layer thickness only has a mild influence on the reduction of the rates of heat and mass transfer. As mentioned before, it is interesting to note that the rate of heat transfer decreases by decreasing the Darcy number. A further decrease in Da then increases the rate of heat transfer. This is clear for $e = 0.8$. This issue is clearly illustrated in Fig. 5.

Based on the above argument, a minimum Nusselt number exists in double diffusive phenomena due to the existence of double boundary layers (solutal and thermal). The minimum in Nu (Sh) is possible if the solutal (thermal) boundary layer is mainly embedded in the porous layer, while thermal (solutal) boundary layer is extended into the pure fluid region. For thermal (or solutally) driven flow it is possible to obtain two peaks in the velocity profiles (Fig. 7(a)) due to flow penetration into the porous layer. However, no inversion in the evolution of the thermal boundary layer is evidence in

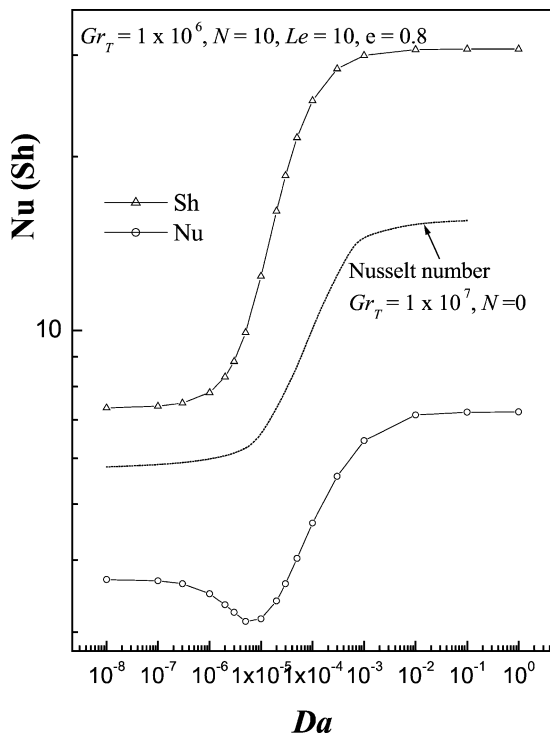


Fig. 5. Dependence of Nu and Sh numbers on the Da for $N = 10$ and $N = 0$ (thermally driven).

Fig. 7(b), i.e., for thermally driven flow no minimum in the rate of heat transfer can be expected, Fig. 5.

4.2. Effect of anisotropy

In several applications, the porous material is anisotropic, such as fiberglass, layered insulator, etc. In general, anisotropic materials have anisotropy in permeability and in thermal, species diffusivities (see for instance [17]). In [17] the effect of anisotropy in the permeability (hydrodynamic anisotropy) is considered.

Changing K^r , i.e., the ratio of K_X to K_Z , addresses the effect of hydraulic anisotropy. It should be mention that when $K^r < 1$ the flow channels in the vertical direction and as $K^r > 1$ the flow channels in the horizontal direction. A new parameter ($Da K^r$) arises in the momentum equation in the anisotropic porous media, hence the transport phenomena in the anisotropic media is more complicated than in the isotropic media case.

Fig. 8(a) and (b) show the effect of Darcy number on the rate of heat transfer and mass transfer, respectively (for $N = 10$). It is evidence that for $Da > 0.01$ (highly permeable region) and for $Da < 5 \times 10^{-7}$ (low permeability region) the effect of anisotropy on the rate of heat and mass transfer is negligible. In fact for $Da < 10^{-6}$, the porous medium is almost impermeable and heat and mass transfer are diffusive. For $Da > 10^{-2}$ (high permeable media), the existence of porous layers does not influence the flow significantly.

The rate of heat transfer (Fig. 8(a)) starts to decrease by increasing Da above 10^{-6} until it reaches a minimum value and then the rate of heat transfer increases by increasing Da .

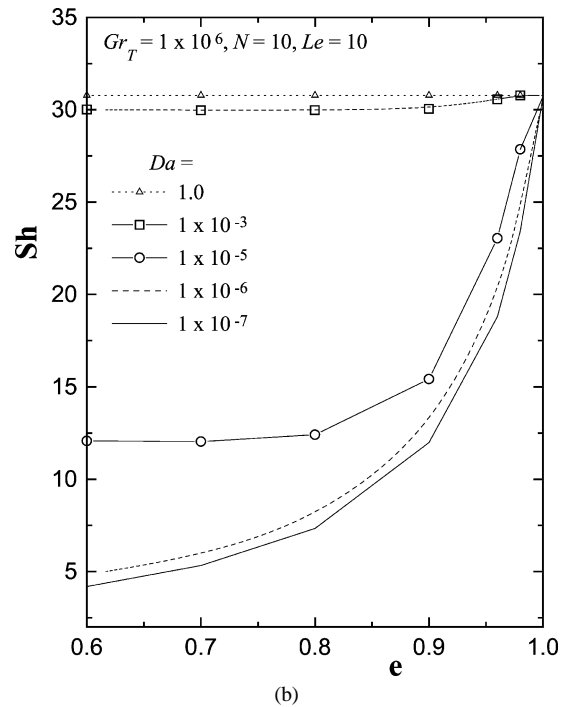
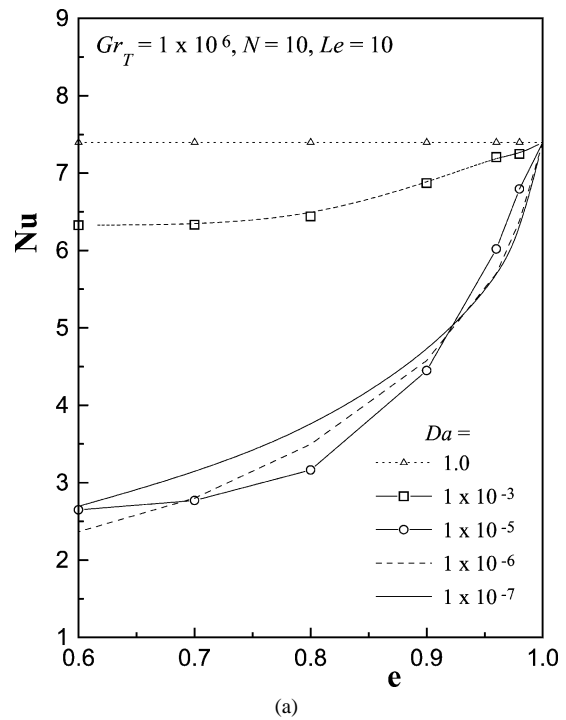
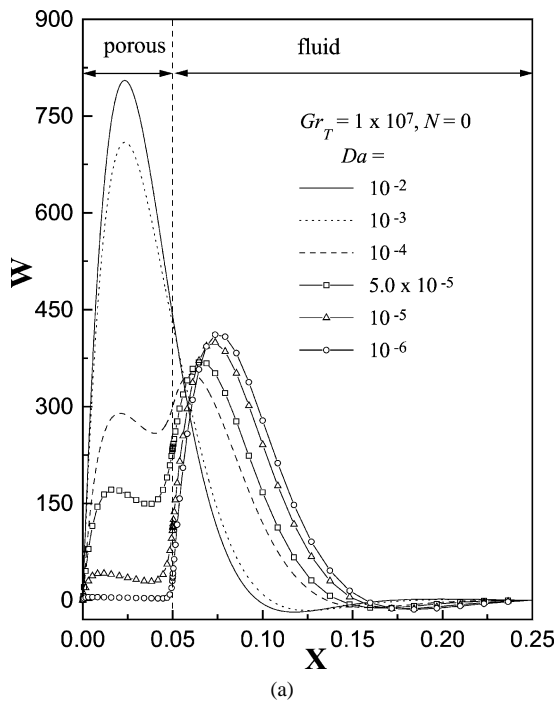
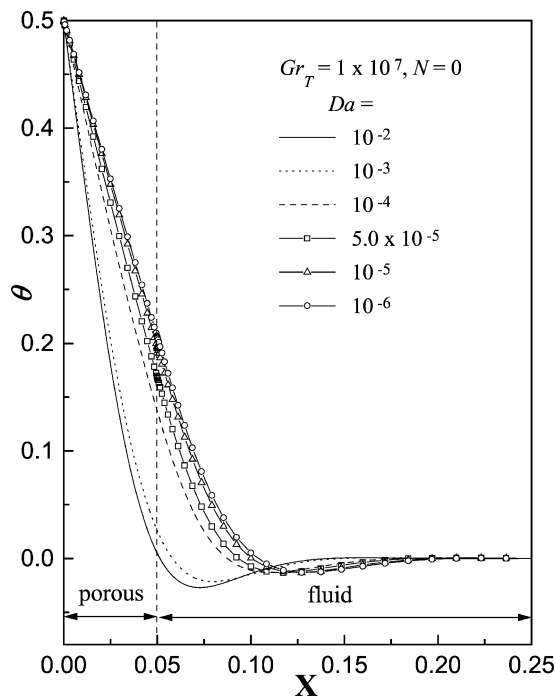


Fig. 6. (a) Nusselt number, and (b) Sherwood number as function of porous layer thickness for different Darcy numbers and for $Gr_T = 10^6$, $N = 10$ and $Le = 10$.

The value of Da at which the minimum Nu value takes place depends on K^r . As K^r decreases Da increases for minimum rate of heat transfer. This is true for $K^r < 1$. For $K^r > 1$, the optimal Da is almost constant ($Da = 8 \times 10^{-6}$). For K^r greater than unity, the flow is only due to vertical porous resistance (vertical channels).



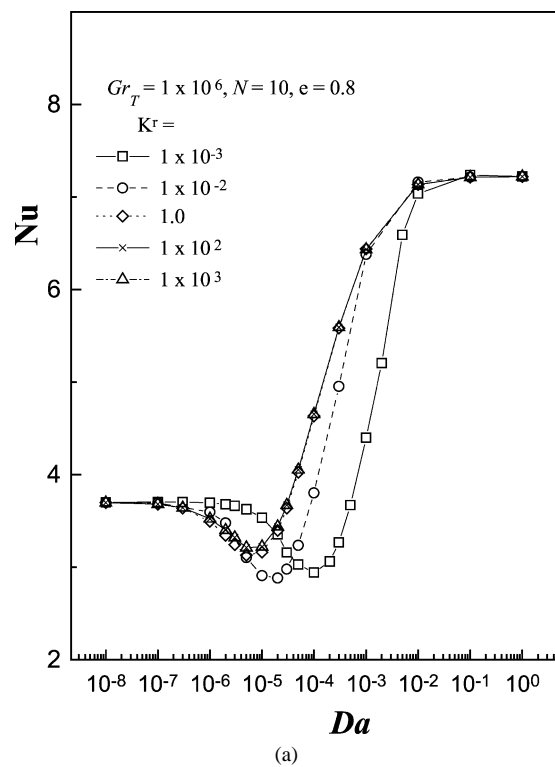
(a)



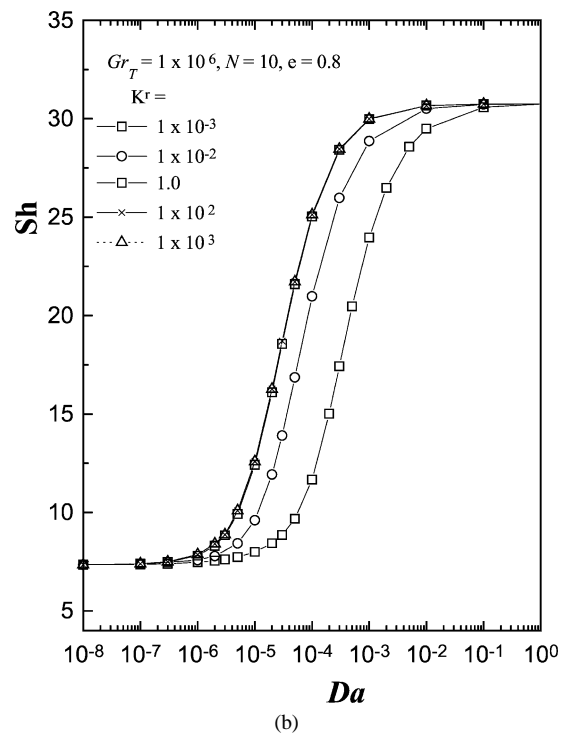
(b)

Fig. 7. (a) W -velocity, and (b) temperature profiles at mid height of the enclosure for thermal driven flow ($N = 0$), $Gr_T = 10^7$ and for different Darcy number.

The principle of minimum rate of heat transfer can be explained on the same bases as discussed for isotropic media. In other words, flow penetration into the porous layer induces heat transfer by the advection mechanism, which is enhanced by solutal buoyancy and consequently reduces the flow intensity in the clear fluid region. The rate of mass



(a)



(b)

Fig. 8. The effects of permeability ratio on (a) the Nusselt number, and (b) the Sherwood number as a function of Darcy number for fixed porous layer thickness.

transfer is not a strong function of the Darcy number and permeability ratios for both the high permeability and the low permeability range of Da ($Da > 10^{-2}$ and $Da < 10^{-6}$). For $10^{-6} < Da < 10^{-2}$ (intermediate permeability range)

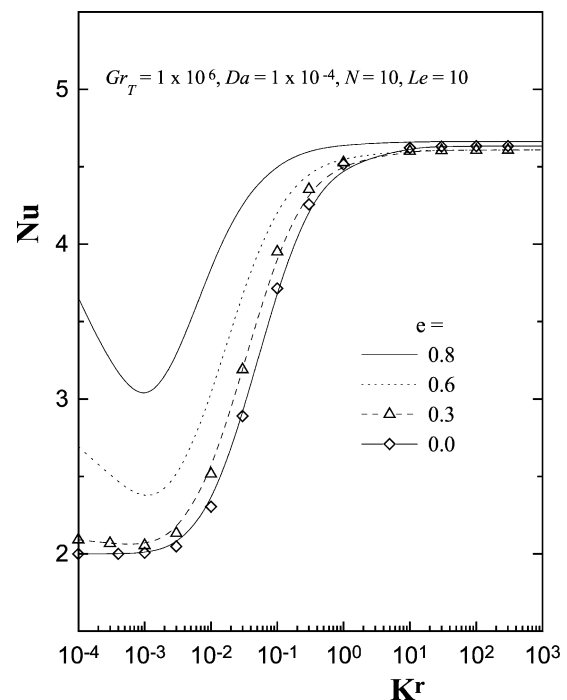
the rate of mass transfer decreases as K^r decreases for the same Darcy number and for K^r less than unity. In fact, it is possible to obtain optimal (minimal) value for mass transfer, if the thermal boundary layer is embedded in the porous layer and solutal boundary layer extended into the pure fluid region.

Fig. 9(a) and (b) show the effect of the permeability ratio on the rate of heat and mass transfer respectively, for different porous layer thicknesses. The figure is for $Da = 10^{-4}$, $Gr_T = 10^6$, $N = 10$ and $Sc = 7.1$. The effect of anisotropy is not that significant for high and low permeability ratios. Therefore for range $10^{-4} < K^r < 1$, for a fixed porous layer, increasing the permeability ratio increases the rate of heat and mass transfer. The rate of heat and mass transfer is mainly controlled by the diffusion mechanism for low permeability ratios. The convection (advection) mechanism increases as the hydraulic anisotropy increases, for high permeability ratios the convection will be the main mechanism of the transport. This is consistent with result of [17]. Their results show that the thermal boundary layer thickness decreases as the permeability ratio increases, i.e., the rate of heat transfer increases with an increase in the permeability ratio. Also, it is evidenced from Fig. 9 that for fixed permeability ratio, the rate of heat and mass transfer decreases as the thickness of the porous layer increases as in the case for isotropic porous layers. The minimal Nu is deeper for porous layer thickness of 0.1 ($e = 0.8$) and the minimal value in Nu diminishes as porous layers become thicker. For thick porous layer, both thermal and solutal boundary layer embedded in the porous layers and the rate of heat and mass transfer is enhanced by the advection mechanism.

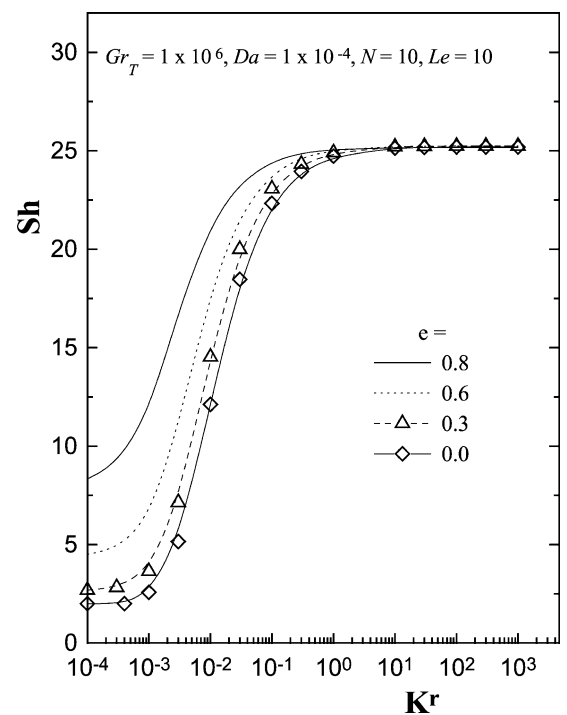
5. Conclusions

Double diffusive, natural convection in a closed, vertical enclosure fitted with two symmetrical porous layers confining a fluid layer is analyzed numerically. The effect of anisotropy on the rate of heat and mass transfer is discussed. A porous layer can be classified into three: low permeability, intermediate and high permeability. The heat and mass transfer are conduction dominated for low permeable porous layer and flow penetration into porous layer is insignificant. The effect of high permeable porous layer on the rate of transport of momentum, heat and mass is minimal. For intermediate permeable region, there is a possibility to obtain a minimum value in the Nusselt number or Sherwood number.

The paper clarifies the physics behind the existence of a minimal Nu , which have been noticed by others and also observed in the present. The optimal (minimum) Nu is a double-diffusive controlled phenomena. The minimum in Nu takes place if the solutal boundary layer is contained in the porous layer while the thermal boundary layer extends into



(a)



(b)

Fig. 9. The effects of porous layer thickness on (a) the Nusselt number, and (b) the Sherwood number as a function of permeability ratio for given Darcy number.

the clear fluid region. Hence, the occurrence of minimal Nu is a function of the porous layer thickness.

Nusselt and Sherwood numbers are not functions of permeability ratio for high and low permeability ratio, i.e., for the range of $10^{-4} > K^r > 1$. The rate of heat and mass

transfer increases as the permeability ratio is varied in the range $10^{-4} < K^r < 1$. The Darcy number at which minimal Nusselt number take places increases as the permeability ratio decreases for K^r less than unity. The Darcy number at which minimal Nu takes place is not a function of K^r for K^r greater than unity.

Acknowledgements

The authors wish to thank the Professor E. LEONARDI for the helpful discussions and the AUPELF-UREF (Agence universitaire de la Francophonie) for the financial support. Also, A.A. Mohamad would like to acknowledge the financial support of the Natural Sciences and Engineering Research Council of Canada (NSERC) through the research grant.

References

- [1] P. Cheng, Heat transfer in geothermal system, *Adv. Heat Transfer* 14 (1979) 1–105.
- [2] D. Nield, A. Bejan, *Convection in Porous Media*, Springer-Verlag, New York, 1992.
- [3] D. Poulikakos, A. Bejan, Natural convection in vertically and horizontally layered porous media heated from the side, *Internat. J. Heat Mass Transfer* 26 (1983) 1805–1814.
- [4] F.C. Lai, F.A. Kulacki, Natural convection across a vertical layered porous cavity, *Internat. J. Heat Mass Transfer* 31 (1988) 1247–1260.
- [5] F. Lauriat, F. Mesguich, Natural convection and radiation in an enclosure partially filled with a porous insulation, *ASME Paper No. 84-WA/HT* (1984) 1–10.
- [6] T.W. Tong, E. Subramanian, Natural convection in rectangular enclosures partially filled with a porous medium, *Internat. J. Heat Fluid Flow* 7 (1986) 3–10.
- [7] C. Beckermann, S. Ramadhyani, R. Viskanta, Natural convection flow and heat transfer between a fluid layer and a porous layer inside a rectangular enclosure, *J. Heat Transfer* 109 (1987) 363–370.
- [8] C. Beckermann, R. Viskanta, S. Ramadhyani, Natural convection in vertical enclosures containing simultaneously fluid and porous layers, *J. Fluid Mech.* 186 (1988) 257–284.
- [9] S.B. Sathé, W.-Q. Lin, T.W. Tong, Natural convection in enclosures containing an insulation with a permeable fluid-porous interface, *Internat. J. Heat Fluid Flow* 9 (1988) 389–395.
- [10] P. Le Breton, J.P. Caltagirone, E. Arquis, Natural convection in a square cavity with thin porous layers on its vertical walls, *J. Heat Transfer* 113 (1991) 892–899.
- [11] D. Gobin, B. Goyeau, J.-P. Songbe, Double diffusive natural convection in a composite fluid-porous layer, *J. Heat Transfer* 120 (1998) 234–242.
- [12] B. Goyeau, D. Gobin, Heat transfer by thermosolutal natural convection in a vertical composite fluid-porous cavity, *Internat. Comm. Heat Mass Transfer* 26 (1999) 1115–1126.
- [13] E. Arquis, J.-P. Caltagirone, Sur les conditions hydrodynamiques au voisinage d'une interface milieu fluide—milieu poreux—application à la convection naturelle, *C. R. Acad. Sci.* 299 (II) (1984) 1–4.
- [14] J.P. Van Doormaal, G.D. Raithby, Enhancements of the SIMPLE method for predicting incompressible fluid flows, *Numer. Heat Transfer* 7 (1984) 147–163.
- [15] A. Tobbal, R. Bennacer, Heat and mass transfer in anisotropic porous layer, *Trends Heat Mass Momentum Transfer* 3 (1997) 129–137.
- [16] O.V. Trevisan, A. Bejan, Natural convection with combined heat and mass transfer buoyancy effects in a porous medium, *Internat. J. Heat Mass Transfer* 28 (1985) 1597–1611.
- [17] R. Bennacer, A. Tobbal, H. Beji, P. Vasseur, Double diffusive convection in a vertical enclosure filled with anisotropic media, *Internat. J. Thermophys. Sci.* 40 (2001) 30–41.